

Chiral quantum batteries

Rong-Fang Liu,^{1,2} Wan-Lu Song,³ Wan-Li Yang,^{2,*} Hua Guan,^{2,†} and Jun-Hong An^{1,‡}

¹Key Laboratory of Quantum Theory and Applications of Ministry of Education, Lanzhou Center for Theoretical Physics, Gansu Provincial Research Center for Basic Disciplines of Quantum Physics, Lanzhou University, Lanzhou 730000, China

²Key Laboratory of Time Reference and Applications, Chinese Academy of Sciences, Innovation Academy for Precision Measurement Science and Technology, Chinese Academy of Sciences, Wuhan 430071, China

³Department of Physics, Hubei University, Wuhan 430062, China

Exploiting quantum effects for energy storage, quantum batteries (QBs) offer compelling advantages over conventional ones in terms of superior energy density, ultrafast charging, and high conversion efficiency. However, their realization is hampered by decoherence, which causes incomplete charging, rapid self-discharging, and reduced extractable work. Here, we propose a QB architecture based on a chiral magnonic platform. It comprises two yttrium iron garnet (YIG) spheres, one serving as the charger and the other as the QB, coupled to a waveguide. The unique chiral coupling between magnons and the guided electromagnetic fields breaks inversion symmetry, inducing both nonreciprocal energy flow and coherent interference between the charger and QB. Their synergy endows our QB with a 34-fold increase in energy capacity and a 55-fold boost in extractable work compared to its achiral counterpart in an experimentally accessible regime. Our scheme harnesses the decoherence from the electromagnetic fields and turns its destruction into an asset, which enables the robustness and wireless-like remote charging features of the QB. Our analysis reveals that these extraordinary capabilities stem from quantum coherence. By establishing chirality as a useful quantum resource, our work paves a viable path toward the realization of QBs.

Introduction.—The growing demand for energy resulting from industrial expansion, population growth and the transition to renewable and miniaturized energy systems makes it urgent to transform conventional energy storage technologies. Quantum batteries (QBs) are an innovative technology that could revolutionize existing battery technologies by using quantum mechanical principles, such as quantum superposition, entanglement, and coherence, in the storage and release of energy [1, 2]. They exhibit remarkable superiority to conventional batteries in terms of increased energy storage capacity [3–5], faster charging rates [6–9], and higher extractable-work efficiency [10–14]. The proof-of-principle experimental realizations of QBs have been demonstrated in the systems of quantum dot [15], trapped ion [16], linear optics [17], and organic microcavity [18].

The practical realization and application of QBs are hindered by ubiquitous decoherence in the microscopic world. Decoherence causes degraded charging efficiency, spontaneous energy loss called self-discharging, and reduced extractable work to QBs. Many strategies have been proposed to overcome these unwanted effects caused by decoherence. It has been found that the ideal efficiency of QBs can be preserved using remote charging mediated by a waveguide [19], topological phases of the reservoir [20, 21], nonreciprocal charging [22–25], non-Hermiticity induced exceptional points [26, 27], non-Markovian effect [28], and noise assisted dissipative charging [11, 29]. Further studies reveal that the self-discharging of QBs can be suppressed by Floquet engineering [30] and enhancing quantum coherence via hyperfine interactions in nitrogen-vacancy centers [31]. Therefore, in the current noisy intermediate-scale quan-

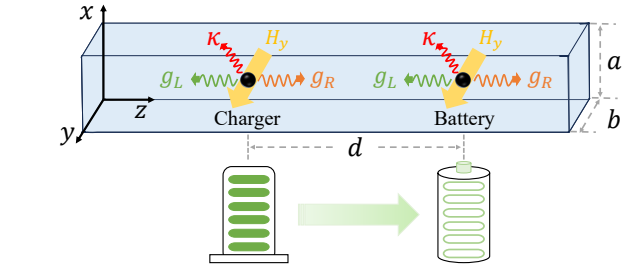


FIG. 1. Schematic of a chiral QB setup. Two YIG spheres separated by a distance d are coupled to a waveguide via the chiral coupling rates $g_{L/R}$ along the z -axis. A static bias magnetic field H_y along the y -axis is applied to produce a uniform eigenfrequency of the magnons in the YIG spheres. κ is the damping rate of the magnons. The left YIG sphere acts as the charger and the right one acts as the QB.

tum era, developing more stable QB architectures with intrinsic robustness to decoherence and uncovering more useful quantum resources to enhance the QB performance in the practical decoherence situation are highly desirable. On the other hand, there is an increasing interest in studying the chiral degrees of freedom that occur in different light-matter interfaces [32–44]. It has become a powerful resource for engineering quantized light-matter interactions, enabling the development of chiral quantum control in giant atom systems [45–48] and quantum interconnect in chiral waveguide- or cavity-QED systems [49–52]. A natural question is whether the chiral degree of freedom of quantum systems can be used to enhance the performance of QBs, especially in the presence of decoherence.

Based on the fact that the eigenenergies of continuous-variable systems are unbounded from above, it is expected that the continuous-variable systems have a greater energy capacity than the discrete-variable systems. Inspired by recent experimental progress on chiral magnon-photon coupling in a spin-momentum locked waveguide [53], we propose a continuous-variable QB scheme consisting of a pair of distant magnons that are chirally coupled to the electromagnetic fields in a waveguide. The chiral interactions result in the breaking of the inversion symmetry, leading to nonreciprocal dissipation and unbalanced coherent interference between the charger and QB. The interplay of these two effects enables our QB to exhibit an enhancement of two orders of magnitude in both of the energy capacity and the extractable work compared to its achiral counterpart, even in the presence of local magnon dissipation. In particular, our QB works flawlessly in a wireless-like remote-charging manner. Our analysis reveals that it is quantum coherence induced by the nonreciprocal dissipation and unbalanced coherent interference that governs the QB performance. Our results demonstrate that chirality can be used as an additional resource to improve the performance of QBs in practical decoherence situations.

Chiral QB scheme.— We propose a continuous-variable chiral QB scheme. It consists of two distant yttrium iron garnet (YIG) spheres embedded in a rectangular hollow metallic waveguide, as shown in Fig. 1. Having a common resonance frequency $\omega_0 = \gamma\mathcal{H}_y$, with $\gamma = 28$ GHz/T being the gyromagnetic ratio and \mathcal{H}_y being the static applied field along y -axis, the magnons generated in the spheres form a continuous-variable quantum two-mode system. The magnon mode of the first YIG sphere serves as the charger and the second one serves as the QB. The energy is supplied to the charger by a classical driving field. The QB and the charger are far separated such that the energy cannot be coherently transferred to the QB. This design can avoid the destructive influence of the local decoherence of the charger and QB on the charging process. The Hamiltonian of the total system is $\hat{H}(t) = \hat{H}_m(t) + \hat{H}_w + \hat{H}_i$, with ($\hbar = 1$)

$$\hat{H}_m(t) = \sum_{j=1,2} \omega_0(\hat{m}_j^\dagger \hat{m}_j + \frac{1}{2}) + \Omega(\hat{m}_1^\dagger e^{-i\omega_d t} + \text{H.c.}), \quad (1)$$

$$\hat{H}_w = \sum_{\lambda=L,R} \int \omega \hat{b}_\lambda^\dagger(\omega) \hat{b}_\lambda(\omega) d\omega, \quad (2)$$

$$\hat{H}_i = \sum_{\lambda=L,R} \int d\omega \left[\frac{ig_{\lambda j}}{\sqrt{2\pi}} \hat{b}_\lambda^\dagger(\omega) \hat{m}_j e^{-i\frac{\omega}{v_\lambda} z_j} + \text{H.c.} \right], \quad (3)$$

where Ω and ω_d are the amplitude and frequency of the driving field, \hat{m}_j and $\mathbf{r}_j = (x_j, z_j)$ are the annihilation operators and the positions of the charger and QB, and $\hat{b}_{L/R}(\omega)$ are the annihilation operators of the left- and right-propagating electromagnetic fields with frequency ω and group velocities $v_{L/R}$ in the wave-

guide. The coupling strength between the j th magnon and the λ -propagating electromagnetic fields is $g_{\lambda j}(\omega) = \mu_0 \sqrt{\frac{\gamma M V_j}{2}} (iB_{x_j}^\lambda - B_{z_j}^\lambda)$, where B_{x_j/z_j}^λ is the magnetic-field strength felt by the j th YIG sphere, μ_0 is the vacuum permeability, M and V_j are the magnetization strength and the volume of the j th YIG sphere. For the TE₁₀ mode, the coupling strength becomes $g_{\lambda j}(\omega) = \sqrt{\frac{\gamma_0 M V_j}{2\epsilon_0 \omega a b}} \left[\frac{\pi}{a} \cos\left(\frac{\pi x_j}{a}\right) - k_\lambda \sin\left(\frac{\pi x_j}{a}\right) \right]$ [54, 55], where a and b are the lengths of the cross section of the waveguide, ϵ_0 is the vacuum permittivity, and $k_\lambda = \omega/v_\lambda$ is the wave vector. We consider that the two YIG spheres have $x_1 = x_2 \equiv x_0$ and $V_1 = V_2 \equiv V$, which reduce $g_{\lambda 1}(\omega) = g_{\lambda 2}(\omega) \equiv g_\lambda(\omega)$. The relation of the two wave vectors as $k_R = -k_L \equiv k$ endows $g_L(\omega) \neq g_R(\omega)$ and thus the chiral feature of the magnon-waveguide coupling. The chirality roots from the elliptically polarized magnetic components giving rise to the so-called spin-momentum locking [35]. We can tune the coupling strength and chirality by the position x_0 of the magnets.

Tracing the degree of freedoms of the common electromagnetic fields in the waveguide from the unitary dynamics of the total system and making the Born-Markov approximation, we derive a master equation satisfied by the density matrix $\rho(t)$ of the charger and the QB as [56]

$$\begin{aligned} \dot{\rho}(t) = & -i[\hat{H}_m(t) + \sum_{\lambda=L,R} \hat{H}_\lambda, \rho(t)] + \left\{ \sum_{\lambda=L,R} \Gamma_\lambda \check{\mathcal{L}}_{\hat{M}_\lambda} \right. \\ & \left. + \sum_{j=1,2} \kappa [(\bar{n} + 1) \check{\mathcal{L}}_{\hat{m}_j} + \bar{n} \check{\mathcal{L}}_{\hat{m}_j^\dagger}] \right\} \rho(t), \quad (4) \end{aligned}$$

where $\Gamma_\lambda = g_\lambda(\omega_0)^2$, κ and $\bar{n} = (e^{\omega_0/k_B T} - 1)^{-1}$ are the identical decay rate and mean thermal excitation number of the two magnons at temperature T , $\check{\mathcal{L}}_{\hat{o}} = \hat{o} \cdot \hat{o}^\dagger - \frac{1}{2} \{ \hat{o}^\dagger \hat{o}, \cdot \}$ is the Lindblad superoperator, and k_B is the Boltzmann's constant. The Hamiltonians $\hat{H}_L = -\frac{i\Gamma_L}{2} (\hat{m}_1^\dagger \hat{m}_2 e^{ik_0 d} - \text{H.c.})$ and $\hat{H}_R = -\frac{i\Gamma_R}{2} (\hat{m}_2^\dagger \hat{m}_1 e^{ik_0 d} - \text{H.c.})$ describe the coherent couplings between the magnons mediated by the left- and right-propagating electromagnetic fields, with $k_0 = \omega_0/v_R$ and $d \equiv |z_1 - z_2|$ [57]. The operators $\hat{M}_L = \hat{m}_1 + \hat{m}_2 e^{ik_0 d}$ and $\hat{M}_R = \hat{m}_1 + \hat{m}_2 e^{-ik_0 d}$ describe the collective dissipations induced by the left- and right-propagating electromagnetic fields in the waveguide, respectively. It is obvious that the chiral coupling due to $g_L(\omega) \neq g_R(\omega)$ causes the breakdown of the inversion symmetry to Eq. (4), which is expected to establish a unidirectional energy channel from the charger to the QB. This nonreciprocity can be quantified by a dimensionless parameter [53]

$$D = (\Gamma_R - \Gamma_L)/(\Gamma_R + \Gamma_L), \quad (5)$$

where $D = 1$ indicates the fully nonreciprocal case and $D = 0$ denotes the reciprocal case. Another feature of our QB is that unbalanced coherent interferences with a phase difference $k_0 d$ between the charger and the QB in

$\hat{H}_L \neq \hat{H}_R$ are induced by the mediation role of the electromagnetic fields in the waveguide. As we will see, the interplay between the nonreciprocity and the coherent interferences endows our QB unprecedented capabilities in energy capacity, extractable work, and remote charging. The nonreciprocity of our system stems from the chiral interaction between the magnons and the electromagnetic field. It is essentially different from the one in Ref. [22], which is from the balance between the QB-charger coherent couplings and their local dissipations.

The performance of our QB is characterized by the following quantities. The first quantity is the stored energy defined as $\mathcal{E}_B(t) = \text{Tr}[\hat{H}_B \rho_2(t)]$ with $\hat{H}_B = \omega_0(\hat{m}_2^\dagger \hat{m}_2 + \frac{1}{2})$ and $\rho_2(t) = \text{Tr}_1[\rho(t)]$ [58–60]. It quantifies the amount of energy stored in the QB. However, according to the second law of thermodynamics, not all of $\mathcal{E}_B(t)$ is convertible into useful work by unitary transformation [12]. Thus, we need a quantity to measure the maximum work that can be extracted from the QB by unitary transformation, i.e., the ergotropy defined as $\mathcal{W}(t) = \mathcal{E}_B(t) - \text{Tr}[\hat{H}_B \tilde{\rho}_2(t)]$ [61, 62]. Here $\tilde{\rho}_2(t)$ is the so-called passive state whose energy is not unitarily extractable [1, 59]. For the continuous-variable system, the Gibbs state has been proven to be the passive state. The work-extraction efficiency of the QB reads $R(t) \equiv \mathcal{W}(t)/\mathcal{E}_B(t)$, which describes the fraction of energy that is convertible into usable work. The third quantity is quantum coherence of the QB defined by the relative entropy $C(t) = \text{Tr}(\rho_2 \log_2 \rho_2) - \text{Tr}(\rho_2 \log_2 \rho_d)$, where ρ_d is the state obtained from ρ_2 by deleting all off-diagonal elements [61, 63]. It has been reported that quantum coherence plays a constructive role in extracting work [13, 61] and mitigating self-discharging [31] of discrete-variable QBs. When ρ_2 is Gaussian, the stored energy, ergotropy, and quantum coherence are [64, 65]

$$\mathcal{E}_B(t) = \omega_0 \{ \text{Tr}[\boldsymbol{\sigma}(t)]/4 + |\mathbf{d}(t)|^2/2 \}, \quad (6)$$

$$\mathcal{W}(t) = \mathcal{E}_B - \omega_0 \sqrt{\det[\boldsymbol{\sigma}(t)]}/2, \quad (7)$$

$$C(t) = \mathcal{S}(\bar{N}) - \mathcal{S}((\sqrt{\det[\boldsymbol{\sigma}(t)]} - 1)/2). \quad (8)$$

Here $\boldsymbol{\sigma}(t)$ and $\mathbf{d}(t)$ are the covariance matrix and displacement vector of $\rho_2(t)$ whose elements are defined as $\sigma_{lm} = \text{Tr}[\{\Delta \hat{r}_l, \Delta \hat{r}_m\} \rho_2(t)]$ and $d_l = \text{Tr}[\hat{r}_l \rho_2(t)]$, with $\Delta \hat{r}_l = \hat{r}_l - d_l$ and $\hat{r} = (\frac{\hat{m}_2 + \hat{m}_2^\dagger}{\sqrt{2}}, \frac{\hat{m}_2 - \hat{m}_2^\dagger}{i\sqrt{2}})^T$, $\mathcal{S}(x) = (x+1) \log_2(x+1) - x \log_2 x$, and $\bar{N} = (\text{Tr}[\boldsymbol{\sigma}(t)] + 2|\mathbf{d}(t)|^2 - 2)/4$. The last quantity is the remote-charging efficiency defined as $\eta(t) = \mathcal{E}_B(t)/\mathcal{E}_C(t)$, where $\mathcal{E}_C(t) = \text{Tr}[\hat{H}_C \rho_1(t)]$ is the charger energy with $\hat{H}_C = \omega_0(\hat{m}_1^\dagger \hat{m}_1 + \frac{1}{2})$ and $\rho_1(t) = \text{Tr}_2[\rho(t)]$. It measures the fraction of the energy that can be remotely transferred from the charger to the QB via the mediation role of the common electromagnetic field in the waveguide. Solving Eq. (4) under the condition of resonant driving $\omega_d = \omega_0$, we derive the steady-state expressions of the energies of the charger

and QB and the ergotropy as [56]

$$\mathcal{E}_{C,ss} = \omega_0 \left[4\Omega^2 \alpha^2 |\zeta|^{-2} + \frac{\kappa \bar{n} \alpha (\xi + 2\Gamma_L^2)}{\xi^2 - 4\Gamma_L^2 \Gamma_R^2} + \frac{1}{2} \right], \quad (9)$$

$$\mathcal{E}_{B,ss} = \omega_0 \left[16\Omega^2 \Gamma_R^2 |\zeta|^{-2} + \frac{\kappa \bar{n} \alpha (\xi + 2\Gamma_R^2)}{\xi^2 - 4\Gamma_L^2 \Gamma_R^2} + \frac{1}{2} \right], \quad (10)$$

$$\mathcal{W}_{ss} = 16\omega_0 \Omega^2 \Gamma_R^2 |\zeta|^{-2}, \quad (11)$$

where $\alpha = \Gamma_L + \Gamma_R + \kappa$, $\zeta = \alpha^2 - 4\Gamma_L \Gamma_R e^{2ik_0 d}$, and $\xi = \alpha^2 - 2\Gamma_L \Gamma_R \cos(2k_0 d)$. The results reveal that, although there is no direct interaction between the charger and the QB, a wireless-like remote charging from the charger to the QB is realized by the L/R -propagating electromagnetic fields in the waveguide via their chiral couplings to the charger and QB. It is remarkable to find that the stored energy $\mathcal{E}_{B,ss}$ is exactly equal to the ergotropy \mathcal{W}_{ss} except for the vacuum zero-point energy when $\bar{n} = 0$. It means that all the energy remotely charged in our scheme is extractable into useful work at zero temperature. This is understandable based on the fact that the passive state is just the vacuum state at the zero temperature. We derive from Eq. (11) that $\max_d \frac{\mathcal{W}_{ss|D=1}}{\mathcal{W}_{ss|D=0}} \approx 64$ when $\kappa/\Gamma_R \ll 1$, which indicates the superiority of our chiral QB over the achiral ones. This result dramatically outperforms the one in Ref. [22], where the enhancement factor in the steady-state storage energy is fourfold.

Numerical results.—Now, we numerically study the explicit performance of our chiral QB. Based on experimentally feasible conditions of our magnon-waveguide setup [54, 55, 66, 67], we choose the parameter values as $\omega_0/2\pi = 16.2$ GHz, $\Gamma_R/2\pi = 20$ MHz, $\kappa/2\pi = 1$ MHz, $\Omega/2\pi = 36$ MHz, and $T = 30$ mK at which $\bar{n} \approx 0$. Our first analysis focuses on how the nonreciprocity governs the charging dynamics of the QB by investigating the QB energy $\mathcal{E}_B(t)$ and the remote-charging efficiency $\eta(t)$. Figure 2(a) shows that, although both the QB and charger experience local decoherence with a rate κ , a stable QB energy is still achieved. It indicates that the electromagnetic fields in the waveguide as a common environment of the charger and QB succeed in mediating a stable energy transfer from the charger to the distant QB, with the destructive impact of their local decoherence sufficiently suppressed. In contrast to the previous scheme where the non-Markovian effect is required [19], our wireless-like remote-charging QB works under the Born-Markov dynamics, which significantly reduces the experimental difficulty in quantum control. Another finding is that $\mathcal{E}_B(t)$ monotonically increases during the whole evolution when D increases from zero to one. Remarkably, the steady-state QB energy $\mathcal{E}_{B,ss}$ when $D = 1$ is about 34 times greater than that when $D = 0$. Note that this factor can be further improved by increasing the driving amplitude Ω [56]. It manifests the powerful charging performance enhanced by the nonreciprocity in our QB scheme. Figure 2(b) reveals a similar monotonic-increasing behavior

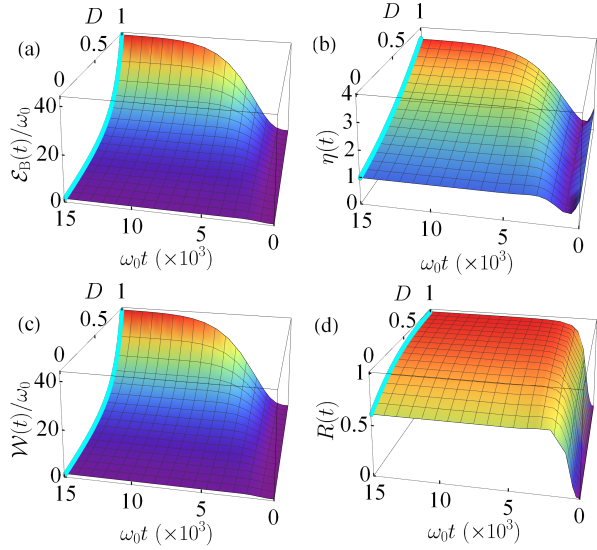


FIG. 2. Evolution of (a) the stored energy $\mathcal{E}_B(t)$, (b) the charging efficiency $\eta(t)$ of the QB, (c) ergotropy, and (d) $R(t)$ as a function of the nonreciprocity parameter D when Γ_L varies from zero to Γ_R . The cyan solid line represents the steady-state analytical solution. The parameters are $k_0 d = \pi/2$, $\omega_d = \omega_0$, $\Omega \approx 0.0022\omega_0$, $\Gamma_R \approx 0.001\omega_0$, $\bar{n} = 0$, and $\kappa = \frac{\Gamma_R}{20}$.

of the charging efficiency $\eta(t)$ with D . The crossover to $\eta(t) > 1$, where the QB energy $\mathcal{E}_B(t)$ exceeds the charger energy $\mathcal{E}_C(t)$, marks a breakdown of reciprocity. This is a direct manifestation of a chirality-directed current that unidirectionally channels the energy from the charger to the QB. It underscores another dominant role played by the chirality in our QB. Figure 2(c) shows that the ergotropy $\mathcal{W}(t)$ evolves to a stable value that monotonically increases with D . A chirality enhanced gain as high as 55 is achieved over the achiral case with $D = 0$. In Fig. 2(d), the work-extraction efficiency $R(t)$ is plotted as a function of D . It monotonically saturates to a value as high as 0.99. It verifies that almost all the QB energy can be converted into useful work in the maximally nonreciprocal case. The numerical results in Fig. 2 exhibit perfect agreement with the analytical steady-state solutions in Eqs. (9)–(11), see the cyan solid lines.

To elucidate the tolerance of the charging efficiency of our chiral QB to the QB-charger distance, we plot in Fig. 3(a) the remote-charging efficiency η_{ss} in the steady state as a function of the nonreciprocity parameter D and the QB-charger distance d . A key observation is that η_{ss} increases monotonically with D while remaining almost independent of d for a large D . Thus, the remote-charging efficiency is solely governed by the nonreciprocity and the coherent interference modulated by the phase $k_0 d$ has a negligible influence on the steady-state energy flux. This result demonstrates that, as far as the charging flux is concerned, our chiral QB works for an arbitrary QB-

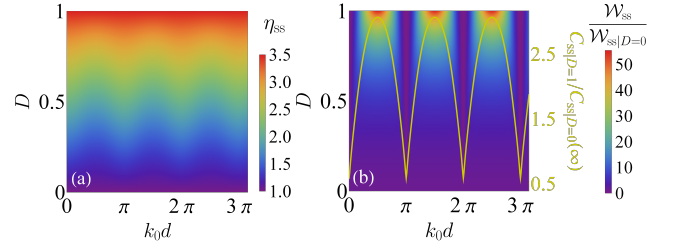


FIG. 3. (a) Charging efficiency η_{ss} and (b) ratio of steady-state ergotropy $\mathcal{W}_{ss}/\mathcal{W}_{ss|D=0}$ as a function of the nonreciprocity parameter D and the QB-charger distance d when Γ_L varies from 0 to Γ_R . The corresponding stable behavior of the quantum coherence $C_{ss|D=1}/C_{ss|D=0}$ is described by the yellow solid lines overlaid on the density plots in (b). The parameters are the same as Fig. 2.

charger distance, which endows our QB with a perfect wireless-like remote-charging capacity. Figure 3(b) further presents the chirality enhanced gain of the steady-state ergotropy with respect to the one in the achiral case, i.e., $\mathcal{W}_{ss}/\mathcal{W}_{ss|D=0}$, with the change of D and d . It exhibits a periodic dependence on d . Its maxima occur at $d = (n + 1/2)\pi/k_0$ and its minima are at $d = n\pi/k_0$, where n is an integer. Notably, under the condition of the largest nonreciprocity $D = 1$, the chirality enhanced gain of the steady-state ergotropy reaches as high as 55 at the constructive-interference distances $d = (n + 1/2)\pi/k_0$ and tends to 1 at the destructive-interference distances $d = n\pi/k_0$. To explain the hidden mechanism, we plot in Fig. 3(b) the ratio $C_{ss|D=1}/C_{ss|D=0}$ between the quantum coherence of $D = 1$ and the one of $D = 0$. It is interesting to find that $\mathcal{W}_{ss}/\mathcal{W}_{ss|D=0}$ is in synchronization with $C_{ss|D=1}/C_{ss|D=0}$. The maxima of the chirality enhanced ergotropy exactly correspond to the ones of quantum coherence. This demonstrates that the quantum coherence plays the dominant role in our chiral QB. This phenomenon stems from a synergy between the nonreciprocity and coherent interference. The nonreciprocity provides the directionality to the energy flow, whereas the coherent interference with the relative phase $k_0 d$ accumulated via the waveguide propagation between the charger and the QB governs the quantum coherence and order of the energy stored in the QB. The interference at $d = n\pi/k_0$ is destructive and does not create quantum coherence. It causes that the stored energy in the QB cannot be converted into useful work. When $d = (n + 1/2)\pi/k_0$, the interference is constructive, generating quantum coherence and allowing the full manifestation of the chirality-induced enhancement of ergotropy. Our results clearly demonstrate the dual role of chirality in regulating QB performance. For the remote-charging efficiency, the nonreciprocity acts primarily as a switch and amplifier of unidirectional energy flow. For the ergotropy, however, the nonreciprocity must cooperate with the spatial quantum interference to determine

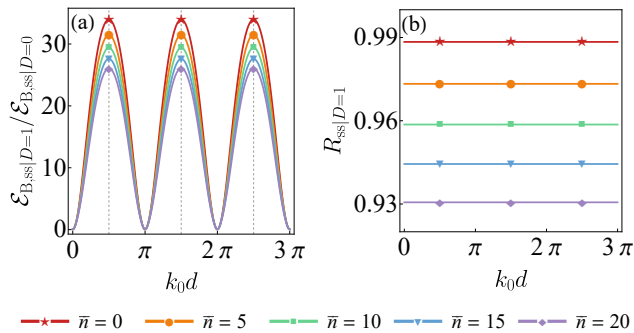


FIG. 4. (a) Chirality enhanced ratio of the steady-state QB energy $\mathcal{E}_{B,ss|D=1}/\mathcal{E}_{B,ss|D=0}$ and (b) $R_{ss|D=1}$ as a function of the QB-charger distance d for different values of \bar{n} . Other parameters are the same as Fig. 2.

the quality of stored energy in the QB. This offers a theoretical insight for the design of high-performance QB based in chiral systems.

Next, we analyze the effect of finite temperature on our scheme. Figure 4(a) shows $\mathcal{E}_{B,ss|D=1}/\mathcal{E}_{B,ss|D=0}$ as a function of the QB-charger distance d for different values of \bar{n} . The enhancement ratio is highest at zero temperature and decreases with increasing \bar{n} . Its periodic dependence on d remains unchanged, which results from quantum coherence and is consistent with the trend in Fig. 3(b). Figure 4(b) presents the steady-state efficiency $R_{ss|D=1}$ as a function of d for various \bar{n} . $R_{ss|D=1}$ decreases as \bar{n} increases. This trend follows from Eqs. (10) and (11): the ergotropy is independent of temperature, whereas the stored energy $\mathcal{E}_{B,ss}$ grows with temperature, thereby reducing $R_{ss|D=1}$ for higher \bar{n} . However, $R_{ss|D=1}$ remains constant with the QB-charger distance, demonstrating that the remote-charging capability of our chiral QB is not degraded by the temperature.

Discussion and conclusion.— Current experimental advances of the chiral waveguide QED provide support for our chiral-QB scheme [39, 40]. Especially, based on the cavity magnonics and waveguide magnonics system [54, 55, 68], a series of integrated platforms have ensured the feasibility of our proposal, such as a ferrimagnetic insulator with high spin density and low damping rates, enabling strong and ultrastrong coupling between magnetostatic modes in YIG spheres and microwave cavity modes [69–76]. Note that experimental observation has confirmed the chiral coupling mechanism in hybrid magnon-altermagnet systems [77, 78]. Being similar to the chiral coupling of emitters to spin-momentum-locked light fields [79, 80], the strong coupling between magnons and photons in a microwave waveguide [81], the negative refractive index effect in photon-magnon hybrid system [82], and the Kittel mode based on ring cavities or waveguides [54, 55, 57, 83] collectively set a solid foundation for the realizability for our scheme.

In conclusion, we have proposed a continuous-variable

chiral QB scheme based on the waveguide magnonics system, where the charger and the QB are formed by two distant YIG spheres embedded in the waveguide. The unique chiral interactions between the magnons of the YIG spheres and the electromagnetic fields in the waveguide induce the nonreciprocity of the energy flow from the charger to the QB and the coherent interference between them without the inversion symmetry. Due to the interplay of these two effects, our QB possesses the capabilities of perfect remote-charging and robustness to the magnon dissipation. The ergotropy of our QB has been found to exhibit a chirality-enhanced gain factor of 55, approaching its theoretical limit of 64, within the experimentally accessible parameter regime. Our analysis reveals that it is the quantum coherence that governs the unprecedented capabilities in energy capacity, remote charging, and maximal extractable work of our QB. Our result establishes chirality as a useful resource for quantum energy management, with implications for quantum thermodynamics devices. With the scalable and tunable framework of waveguide magnonics system, our scheme is extendable to multi-magnon scenarios, providing a useful platform for the practical realization of large-scale QBs.

The work is supported by the Quantum Science and Technology-National Science and Technology Major Project (Grants No. 2023ZD0300404 and No. 2023ZD0300904), the National Natural Science Foundation of China (Grants No. 12275109, No. 92576202, No. 12274422, No. U25A20196, and No. 12247101), the Natural Science Foundation of Hubei Province (2022CFA013), and the Natural Science Foundation of Gansu Province (Grants No. 22JR5RA389 and No. 25JRRA799).

* ywl@wipm.ac.cn

† guanhua@apm.ac.cn

‡ anjhong@lzu.edu.cn

- [1] R. Alicki and M. Fannes, Entanglement boost for extractable work from ensembles of quantum batteries, *Phys. Rev. E* **87**, 042123 (2013).
- [2] F. Campaioli, S. Gherardini, J. Q. Quach, M. Polini, and G. M. Andolina, Colloquium: Quantum batteries, *Rev. Mod. Phys.* **96**, 031001 (2024).
- [3] L. Gao, C. Cheng, W.-B. He, R. Mondaini, X.-W. Guan, and H.-Q. Lin, Scaling of energy and power in a large quantum battery-charger model, *Phys. Rev. Res.* **4**, 043150 (2022).
- [4] X. Yang, Y.-H. Yang, M. Alimuddin, R. Salvia, S.-M. Fei, L.-M. Zhao, S. Nimmrichter, and M.-X. Luo, Battery capacity of energy-storing quantum systems, *Phys. Rev. Lett.* **131**, 030402 (2023).
- [5] T. Zhang, H. Yang, and S.-M. Fei, Local-projective-measurement-enhanced quantum battery capacity, *Phys. Rev. A* **109**, 042424 (2024).
- [6] F. Campaioli, F. A. Pollock, F. C. Binder, L. Céleri, J. Goold, S. Vinjanampathy, and K. Modi, Enhancing the

- charging power of quantum batteries, *Phys. Rev. Lett.* **118**, 150601 (2017).
- [7] D. Ferraro, M. Campisi, G. M. Andolina, V. Pellegrini, and M. Polini, High-power collective charging of a solid-state quantum battery, *Phys. Rev. Lett.* **120**, 117702 (2018).
- [8] D. Rossini, G. M. Andolina, D. Rosa, M. Carrega, and M. Polini, Quantum advantage in the charging process of sachdev-ye-kitaev batteries, *Phys. Rev. Lett.* **125**, 236402 (2020).
- [9] J.-Y. Gyhm, D. Šafránek, and D. Rosa, Quantum charging advantage cannot be extensive without global operations, *Phys. Rev. Lett.* **128**, 140501 (2022).
- [10] G. M. Andolina, M. Keck, A. Mari, M. Campisi, V. Giovannetti, and M. Polini, Extractable work, the role of correlations, and asymptotic freedom in quantum batteries, *Phys. Rev. Lett.* **122**, 047702 (2019).
- [11] F. Barra, Dissipative charging of a quantum battery, *Phys. Rev. Lett.* **122**, 210601 (2019).
- [12] J. Monsel, M. Fellous-Asiani, B. Huard, and A. Auffèves, The energetic cost of work extraction, *Phys. Rev. Lett.* **124**, 130601 (2020).
- [13] H.-L. Shi, S. Ding, Q.-K. Wan, X.-H. Wang, and W.-L. Yang, Entanglement, coherence, and extractable work in quantum batteries, *Phys. Rev. Lett.* **129**, 130602 (2022).
- [14] S. Tirone, R. Salvia, S. Chessa, and V. Giovannetti, Work extraction processes from noisy quantum batteries: The role of nonlocal resources, *Phys. Rev. Lett.* **131**, 060402 (2023).
- [15] I. Maillette de Buy Wenniger, S. E. Thomas, M. Maffei, S. C. Wein, M. Pont, N. Belabas, S. Prasad, A. Harouri, A. Lemaître, I. Sagnes, N. Somaschi, A. Auffèves, and P. Senellart, Experimental analysis of energy transfers between a quantum emitter and light fields, *Phys. Rev. Lett.* **131**, 260401 (2023).
- [16] J. Zhang, P. Wang, W. Chen, Z. Cai, M. Qiao, R. Li, Y. Huang, H. Tian, C. Luan, H. Tu, K. Cui, L. Yan, J. Zhang, J. Zhang, M. Yung, and K. Kim, Single-ion information engine for charging quantum battery, *Phys. Rev. Lett.* **135**, 140403 (2025).
- [17] G. Zhu, Y. Chen, Y. Hasegawa, and P. Xue, Charging quantum batteries via indefinite causal order: Theory and experiment, *Phys. Rev. Lett.* **131**, 240401 (2023).
- [18] J. Q. Quach, K. E. McGhee, L. Ganzer, D. M. Rouse, B. W. Lovett, E. M. Gauger, J. Keeling, G. Cerullo, D. G. Lidzey, and T. Virgili, Superabsorption in an organic microcavity: Toward a quantum battery, *Sci. Adv.* **8**, eabk3160 (2022).
- [19] W.-L. Song, H.-B. Liu, B. Zhou, W.-L. Yang, and J.-H. An, Remote charging and degradation suppression for the quantum battery, *Phys. Rev. Lett.* **132**, 090401 (2024).
- [20] Z.-G. Lu, G. Tian, X.-Y. Lü, and C. Shang, Topological quantum batteries, *Phys. Rev. Lett.* **134**, 180401 (2025).
- [21] S. Cavazzoni, G. Ragazzi, P. Bordone, and M. G. A. Paris, Quantum walks as a tool to design robust quantum batteries: The role of topology and chirality, *Advanced Quantum Technologies* **9**, e00897 (2026).
- [22] B. Ahmadi, P. Mazurek, P. Horodecki, and S. Barzanjeh, Nonreciprocal quantum batteries, *Phys. Rev. Lett.* **132**, 210402 (2024).
- [23] C.-Z. Sun, Z.-K. Wang, W.-B. Yan, Y.-J. Zhang, Z.-X. Man, and Q.-Y. Cai, Nonreciprocal charging in a quantum battery via a mediator, *Phys. Rev. A* **112**, 012429 (2025).
- [24] N. A. Khan, X. Zhang, C. Huang, Y. Liu, and D. He, Collective enhancement in nonreciprocal multimode quantum batteries, *Phys. Rev. B* **112**, 104318 (2025).
- [25] H.-W. Zhao, Y. Xie, X. Huang, and G.-F. Zhang, Enhanced charging in multibattery systems by nonreciprocity, *Phys. Rev. A* **112**, 022214 (2025).
- [26] T. K. Konar, L. G. C. Lakkuraju, and A. Sen (De), Quantum battery with non-hermitian charging, *Phys. Rev. A* **109**, 042207 (2024).
- [27] F.-M. Yang and F.-Q. Dou, Wireless energy transfer in a non-hermitian quantum battery, *Phys. Rev. A* **112**, 042205 (2025).
- [28] F. H. Kamin, F. T. Tabesh, S. Salimi, F. Kheirandish, and A. C. Santos, Non-markovian effects on charging and self-discharging process of quantum batteries, *New Journal of Physics* **22**, 083007 (2020).
- [29] S. Ghosh, T. Chanda, S. Mal, and A. Sen(De), Fast charging of a quantum battery assisted by noise, *Phys. Rev. A* **104**, 032207 (2021).
- [30] S.-Y. Bai and J.-H. An, Floquet engineering to reactivate a dissipative quantum battery, *Phys. Rev. A* **102**, 060201 (2020).
- [31] W.-L. Song, J.-L. Wang, B. Zhou, W.-L. Yang, and J.-H. An, Self-discharging mitigated quantum battery, *Phys. Rev. Lett.* **135**, 020405 (2025).
- [32] J. Petersen, J. Volz, and A. Rauschenbeutel, Chiral nanophotonic waveguide interface based on spin-orbit interaction of light, *Science* **346**, 67 (2014).
- [33] T. Ramos, H. Pichler, A. J. Daley, and P. Zoller, Quantum spin dimers from chiral dissipation in cold-atom chains, *Phys. Rev. Lett.* **113**, 237203 (2014).
- [34] I. Söllner, S. Mahmoodian, S. L. Hansen, L. Midolo, A. Javadi, G. Kiršanskė, T. Pregolato, H. El-Ella, E. H. Lee, J. D. Song, *et al.*, Deterministic photon-emitter coupling in chiral photonic circuits, *Nature Nanotech* **10**, 775 (2015).
- [35] P. Lodahl, S. Mahmoodian, S. Stobbe, A. Rauschenbeutel, P. Schneeweiss, J. Volz, H. Pichler, and P. Zoller, Chiral quantum optics, *Nature* **541**, 473 (2017).
- [36] J. C. Owens, M. G. Panetta, B. Saxberg, G. Roberts, S. Chakram, R. Ma, A. Vrajitoarea, J. Simon, and D. I. Schuster, Chiral cavity quantum electrodynamics, *Nature Physics* **18**, 1048 (2022).
- [37] X. Zhang, Y. Liu, J. Han, Y. Kivshar, and Q. Song, Chiral emission from resonant metasurfaces, *Science* **377**, 1215 (2022).
- [38] Z. Zhang, Z. Xu, R. Huang, X. Lu, F. Zhang, D. Li, c. K. Özdemir, F. Nori, H. Bao, Y. Xiao, B. Chen, H. Jing, and H. Shen, Chirality-induced quantum non-reciprocity, *Nature Photonics* **19**, 840 (2025).
- [39] Y.-X. Zhang, C. R. i Carceller, M. Kjaergaard, and A. S. Sørensen, Charge-noise insensitive chiral photonic interface for waveguide circuit qed, *Phys. Rev. Lett.* **127**, 233601 (2021).
- [40] B. Windt, M. Bello, D. Malz, and J. I. Cirac, Effects of retardation on many-body superradiance in chiral waveguide qed, *Phys. Rev. Lett.* **134**, 173601 (2025).
- [41] S.-H. Gong, F. Alpeggiani, B. Sciacca, E. C. Garnett, and L. Kuipers, Nanoscale chiral valley-photon interface through optical spin-orbit coupling, *Science* **359**, 443 (2018).
- [42] E. Sánchez-Burillo, C. Wan, D. Zueco, and A. González-Tudela, Chiral quantum optics in photonic sawtooth lat-

- tices, *Phys. Rev. Res.* **2**, 023003 (2020).
- [43] R. J. Valencia-Tortora, N. Pancotti, M. Fleischhauer, H. Bernien, and J. Marino, Rydberg platform for non-ergodic chiral quantum dynamics, *Phys. Rev. Lett.* **132**, 223201 (2024).
- [44] Z.-G. Lu, Y. Wu, and X.-Y. Lü, Chiral interaction induced near-perfect photon blockade, *Phys. Rev. Lett.* **134**, 013602 (2025).
- [45] X. Wang, T. Liu, A. F. Kockum, H.-R. Li, and F. Nori, Tunable chiral bound states with giant atoms, *Phys. Rev. Lett.* **126**, 043602 (2021).
- [46] F. Roccati and D. Cilluffo, Controlling markovianity with chiral giant atoms, *Phys. Rev. Lett.* **133**, 063603 (2024).
- [47] Y. Chang, Non-markovian multiphoton chiral dynamics with giant systems, *Communications Physics* **8**, 385 (2025).
- [48] Y.-T. Chen, L. Du, L. Guo, Z. Wang, Y. Zhang, Y. Li, and J.-H. Wu, Nonreciprocal and chiral single-photon scattering for giant atoms, *Communications Physics* **5**, 215 (2022).
- [49] A. Almanakly, B. Yankelevich, M. Hays, B. Kannan, R. Assouly, A. Greene, M. Gingras, B. M. Niedzielski, H. Stickler, M. E. Schwartz, K. Serniak, J. Ī.-j. Wang, T. P. Orlando, S. Gustavsson, J. A. Grover, and W. D. Oliver, Deterministic remote entanglement using a chiral quantum interconnect, *Nature Physics* **21**, 825 (2025).
- [50] E. M. González-Ruiz, F. T. Østfeldt, R. Uppu, P. Lodahl, and A. S. Sørensen, Entanglement properties of a quantum-dot biexciton cascade in a chiral nanophotonic waveguide, *Phys. Rev. A* **108**, 013507 (2023).
- [51] I. M. Mirza and J. C. Schotland, Multiqubit entanglement in bidirectional-chiral-waveguide qed, *Phys. Rev. A* **94**, 012302 (2016).
- [52] F. T. Østfeldt, E. M. González-Ruiz, N. Hauff, Y. Wang, A. D. Wieck, A. Ludwig, R. Schott, L. Midolo, A. S. Sørensen, R. Uppu, and P. Lodahl, On-demand source of dual-rail photon pairs based on chiral interaction in a nanophotonic waveguide, *PRX Quantum* **3**, 020363 (2022).
- [53] J. Qian, Q. Hong, Z.-Y. Wang, W.-X. Wu, Y. Yang, C.-M. Hu, J.-Q. You, and Y.-P. Wang, Unidirectional perfect absorption induced by chiral coupling in spin-momentum locked waveguide magnonics, *Nature Communications* **16**, 8100 (2025).
- [54] T. Yu, Y.-X. Zhang, S. Sharma, X. Zhang, Y. M. Blanter, and G. E. W. Bauer, Magnon accumulation in chirally coupled magnets, *Phys. Rev. Lett.* **124**, 107202 (2020).
- [55] T. Yu, X. Zhang, S. Sharma, Y. M. Blanter, and G. E. W. Bauer, Chiral coupling of magnons in waveguides, *Phys. Rev. B* **101**, 094414 (2020).
- [56] See the Supplemental Material for the detailed derivation of the master equation, the dynamical solution, the forms of energies and ergotropy of the QB, and the effect of the driving strength on the the stored energy of the QB.
- [57] H. Zhan, L. Sun, and H. Tan, Chirality-induced one-way quantum steering between two waveguide-mediated ferromagnetic microspheres, *Phys. Rev. B* **106**, 104432 (2022).
- [58] A. E. Allahverdyan, R. Balian, and T. M. Nieuwenhuizen, Maximal work extraction from finite quantum systems, *Europhysics Letters* **67**, 565 (2004).
- [59] D. Farina, G. M. Andolina, A. Mari, M. Polini, and V. Giovannetti, Charger-mediated energy transfer for quantum batteries: An open-system approach, *Phys. Rev. B* **99**, 035421 (2019).
- [60] D. Šafránek, D. Rosa, and F. C. Binder, Work extraction from unknown quantum sources, *Phys. Rev. Lett.* **130**, 210401 (2023).
- [61] G. Francica, F. C. Binder, G. Guarnieri, M. T. Mitchison, J. Goold, and F. Plastina, Quantum coherence and ergotropy, *Phys. Rev. Lett.* **125**, 180603 (2020).
- [62] B. Çakmak, Ergotropy from coherences in an open quantum system, *Phys. Rev. E* **102**, 042111 (2020).
- [63] T. Baumgratz, M. Cramer, and M. B. Plenio, Quantifying coherence, *Phys. Rev. Lett.* **113**, 140401 (2014).
- [64] S. Tirone, R. Salvia, and V. Giovannetti, Quantum energy lines and the optimal output ergotropy problem, *Phys. Rev. Lett.* **127**, 210601 (2021).
- [65] J. Xu, Quantifying coherence of gaussian states, *Phys. Rev. A* **93**, 032111 (2016).
- [66] B. Yao, T. Yu, Y. S. Gui, J. W. Rao, Y. T. Zhao, W. Lu, and C.-M. Hu, Coherent control of magnon radiative damping with local photon states, *Commun. Phys.* **2**, 161 (2019).
- [67] Y. Kang, X. Zeng, W. Zhang, C. Sun, C. Wu, and G. Wang, *Magnonic entanglement in a chiral cavity-magnon coupling system* (2025), arXiv:2505.16395 [quant-ph].
- [68] F. Pirmoradian, M. Miri, B. Z. Rameshti, and S. Saeidian, Topological magnon modes of a chain of magnetic spheres in a waveguide, *Phys. Rev. B* **107**, 064401 (2023).
- [69] X. Zhang, C.-L. Zou, L. Jiang, and H. X. Tang, Strongly coupled magnons and cavity microwave photons, *Phys. Rev. Lett.* **113**, 156401 (2014).
- [70] Y.-P. Wang, G.-Q. Zhang, D. Zhang, T.-F. Li, C.-M. Hu, and J. Q. You, Bistability of cavity magnon polaritons, *Phys. Rev. Lett.* **120**, 057202 (2018).
- [71] Y.-P. Wang, J. W. Rao, Y. Yang, P.-C. Xu, Y. S. Gui, B. M. Yao, J. Q. You, and C.-M. Hu, Nonreciprocity and unidirectional invisibility in cavity magnonics, *Phys. Rev. Lett.* **123**, 127202 (2019).
- [72] H. Y. Yuan, P. Yan, S. Zheng, Q. Y. He, K. Xia, and M.-H. Yung, Steady bell state generation via magnon-photon coupling, *Phys. Rev. Lett.* **124**, 053602 (2020).
- [73] Y. Li, V. G. Yefremenko, M. Lisovenko, C. Trevillian, T. Polakovic, T. W. Cecil, P. S. Barry, J. Pearson, R. Divan, V. Tyberkevych, C. L. Chang, U. Welp, W.-K. Kwok, and V. Novosad, Coherent coupling of two remote magnonic resonators mediated by superconducting circuits, *Phys. Rev. Lett.* **128**, 047701 (2022).
- [74] Y. Yang, J. Yao, Y. Xiao, P.-T. Fong, H.-K. Lau, and C.-M. Hu, Anomalous long-distance coherence in critically driven cavity magnonics, *Phys. Rev. Lett.* **132**, 206902 (2024).
- [75] J. Yao, C. Lu, X. Fan, D. Xue, G. E. Bridges, and C.-M. Hu, Nonreciprocal control of the speed of light using cavity magnonics, *Phys. Rev. Lett.* **134**, 196904 (2025).
- [76] Z.-Q. Wang, Z.-Y. Wang, Y.-P. Wang, and J. Q. You, Single-mode magnon-polariton lasing and amplification controlled by dissipative coupling, *Phys. Rev. Lett.* **135**, 186704 (2025).
- [77] Z. Jin, T. Gong, J. Liu, H. Yang, Z. Zeng, Y. Cao, and P. Yan, Strong coupling of chiral magnons in altermagnets, *Phys. Rev. Lett.* **135**, 126702 (2025).
- [78] Q. Sun, J. Guo, D. Wang, D. L. Abernathy, W. Tian, and C. Li, Observation of chiral magnon band splitting in altermagnetic hematite, *Phys. Rev. Lett.* **135**, 186703 (2025).
- [79] R. Coles, D. Price, J. Dixon, B. Royall, E. Clarke, P. Kok,

- M. Skolnick, A. Fox, and M. Makhonin, Chirality of nanophotonic waveguide with embedded quantum emitter for unidirectional spin transfer, *Nature communications* **7**, 11183 (2016).
- [80] E. Will, L. Masters, A. Rauschenbeutel, M. Scheucher, and J. Volz, Coupling a single trapped atom to a whispering-gallery-mode microresonator, *Phys. Rev. Lett.* **126**, 233602 (2021).
- [81] V. Demidov, S. Urazhdin, G. de Loubens, O. Klein, V. Cros, A. Anane, and S. Demokritov, Magnetization oscillations and waves driven by pure spin currents, *Phys. Rep.* **673**, 1 (2017).
- [82] J. Kim, B. Kim, and S.-K. Kim, Microwave negative refractive index enabled by anti-parity-time symmetry in a coupled photon-magnon hybrid system, *Phys. Rev. Lett.* **135**, 116905 (2025).
- [83] J. Bourhill, W. Yu, V. Vlamincck, G. E. W. Bauer, G. Ruoso, and V. Castel, Generation of circulating cavity magnon polaritons, *Phys. Rev. Appl.* **19**, 014030 (2023).

Supplemental Material for “Chiral quantum batteries”

Rong-Fang Liu,^{1,2} Wan-Lu Song^{①,3}, Wan-Li Yang,^{2,*} Hua Guan,^{2,†} and Jun-Hong An^{①,‡}

¹Key Laboratory of Quantum Theory and Applications of Ministry of Education, Lanzhou Center for Theoretical Physics, Gansu Provincial Research Center for Basic Disciplines of Quantum Physics, Lanzhou University, Lanzhou 730000, China

²Key Laboratory of Time Reference and Applications, Chinese Academy of Sciences, Innovation Academy for Precision Measurement Science and Technology, Chinese Academy of Sciences, Wuhan 430071, China

³Department of Physics, Hubei University, Wuhan 430062, China

In this supplemental material, we give the detailed derivation of the master equation, the dynamical solution, the forms of energies and ergotropy of the quantum battery (QB), and the effect of the driving strength on the the stored energy of the QB.

I. MASTER EQUATION

The total system consists of the two magnon modes under classical driving, the electromagnetic fields in the waveguide, and two thermal environments felt by the magnon modes. Their free Hamiltonian is

$$\begin{aligned} \hat{H}_0 = & \sum_{j=1,2} [\omega_0(\hat{m}_j^\dagger \hat{m}_j + \frac{1}{2}) + \int \omega \hat{c}_j^\dagger(\omega) \hat{c}_j(\omega) d\omega] \\ & + \sum_{\lambda=L,R} \int \omega \hat{b}_\lambda^\dagger(\omega) \hat{b}_\lambda(\omega) d\omega, \end{aligned} \quad (1)$$

where \hat{m}_j and $\hat{c}_j(\omega)$ are the annihilation operators of the j th magnon and its environment and $\hat{b}_\lambda(\omega)$ is the annihilation operator of the λ -propagating electromagnetic field in the waveguide. The interaction Hamiltonian of the two magnons with electromagnetic fields and the environments in the interaction picture with respect to \hat{H}_0 is $\hat{H}^I(t) = \hat{H}_d(t) + \hat{H}'(t)$, where

$$\hat{H}'(t) = \hat{H}_F(t) + \hat{H}_E(t), \quad (2)$$

$$\hat{H}_d(t) = \Omega[\hat{m}_1^\dagger e^{-i(\omega_d - \omega_0)t} + \text{H.c.}], \quad (3)$$

$$\begin{aligned} \hat{H}_F(t) = & \sum_{\substack{\lambda=L,R \\ j=1,2}} \int \frac{id\omega}{\sqrt{2\pi}} [g_{\lambda j}(\omega) \hat{b}_\lambda^\dagger(\omega) \hat{m}_j e^{i(\omega - \omega_0)t - \frac{i\omega z_j}{v_\lambda}} \\ & - \text{H.c.}], \end{aligned} \quad (4)$$

$$\hat{H}_E(t) = \sum_{j=1,2} \int \frac{id\omega}{\sqrt{2\pi}} [\chi(\omega) \hat{c}_j^\dagger(\omega) \hat{m}_j e^{i(\omega - \omega_0)t} - \text{H.c.}] \quad (5)$$

The electromagnetic fields are initially in the vacuum state and the environments are initially in the thermal state at a finite temperature, i.e., $\rho_F = \prod_{\lambda,\omega} |0_\lambda(\omega)\rangle\langle 0_\lambda(\omega)|$ and

$\rho_E = \prod_j \exp[-\int \omega \hat{c}_j^\dagger(\omega) \hat{c}_j(\omega) / (k_B T) d\omega] / Z$. Therefore, we have the expectation values of the operators in the initial state as

$$\text{Tr}_F[\hat{b}_\lambda(\omega) \rho_F] = \text{Tr}_E[\hat{c}_j(\omega) \rho_E] = 0, \quad (6)$$

$$\text{Tr}_F[\hat{b}_\lambda^\dagger(\omega) \hat{b}_{\lambda'}(\omega') \rho_F] = \text{Tr}_F[\hat{b}_\lambda(\omega) \hat{b}_{\lambda'}^\dagger(\omega') \rho_F] = 0, \quad (7)$$

$$\text{Tr}_F[\hat{b}_\lambda(\omega) \hat{b}_{\lambda'}^\dagger(\omega') \rho_F] = \delta(\omega - \omega') \delta_{\lambda,\lambda'}, \quad (8)$$

$$\text{Tr}_E[\hat{c}_j^\dagger(\omega) \hat{c}_{j'}(\omega') \rho_E] = \text{Tr}_E[\hat{c}_j(\omega) \hat{c}_{j'}^\dagger(\omega') \rho_E] = 0, \quad (9)$$

$$\text{Tr}_E[\hat{c}_j(\omega) \hat{c}_{j'}^\dagger(\omega') \rho_E] = (\bar{n}_\omega + 1) \delta(\omega - \omega') \delta_{j,j'}, \quad (10)$$

$$\text{Tr}_E[\hat{c}_j^\dagger(\omega) \hat{c}_{j'}(\omega') \rho_E] = \bar{n}_\omega \delta(\omega - \omega') \delta_{j,j'}, \quad (11)$$

where $\bar{n}_\omega = [e^{\omega/(k_B T)} - 1]^{-1}$. The Liouville equation of the total system is $\dot{\tilde{\rho}}_{\text{tot}}(t) = -i[\hat{H}_d(t) + \hat{H}'(t), \tilde{\rho}_{\text{tot}}(t)]$ under the initial condition $\tilde{\rho}_{\text{tot}}(0) = \rho_F(0) \rho_E \rho(0)$. Substituting its formal solution $\tilde{\rho}_{\text{tot}}(t) = \tilde{\rho}_{\text{tot}}(0) - i \int_0^t d\tau [\hat{H}_d(\tau) + \hat{H}'(\tau), \tilde{\rho}_{\text{tot}}(\tau)]$ back into it and tracing the degrees of freedom of the electromagnetic fields and the environments, we have

$$\begin{aligned} \dot{\tilde{\rho}}(t) = & -i[\hat{H}_d(t), \tilde{\rho}(t)] - \text{Tr}_{F,E} \int_0^t d\tau \\ & \times [\hat{H}'(t), [\hat{H}_d(\tau) + \hat{H}'(\tau), \tilde{\rho}_{\text{tot}}(\tau)]], \end{aligned} \quad (12)$$

where $\tilde{\rho}(t) = \text{Tr}_{F,E}[\tilde{\rho}_{\text{tot}}(t)]$. Under the Born approximation, the state $\tilde{\rho}_{\text{tot}}(\tau)$ would factor as a direct product $\tilde{\rho}_{\text{tot}}(\tau) \simeq \tilde{\rho}(\tau) \rho_F(0) \rho_E(0)$. Furthermore, under the Markov approximation, we can replace $\tilde{\rho}(\tau)$ by $\tilde{\rho}(t)$. Equation (12) is converted into [1]

$$\begin{aligned} \dot{\tilde{\rho}}(t) = & -i[\hat{H}_d(t), \tilde{\rho}(t)] - \text{Tr}_{F,E} \int_0^t d\tau \\ & \times [\hat{H}'(t), [\hat{H}'(\tau), \tilde{\rho}(t) \rho_F \rho_E]], \end{aligned} \quad (13)$$

where Eq. (6) has been used.

Substituting Eq. (2) into Eq. (13), we rewrite the last term of Eq. (13) as $Q_1 + Q_2 + Q_3$, where

$$Q_1 = -\text{Tr}_{F,E} \int_0^t d\tau [H_F(t), [H_F(\tau), \tilde{\rho}(t) \rho_F \rho_E]], \quad (14)$$

$$Q_2 = -\text{Tr}_{F,E} \int_0^t d\tau [\hat{H}_E(t), [\hat{H}_E(\tau), \tilde{\rho}(t) \rho_F \rho_E]], \quad (15)$$

$$\begin{aligned} Q_3 = & -\text{Tr}_{F,E} \int_0^t d\tau \{ [\hat{H}_F(t), [\hat{H}_E(\tau), \tilde{\rho}(t) \rho_F \rho_E]] \\ & + [\hat{H}_E(t), [\hat{H}_F(\tau), \tilde{\rho}(t) \rho_F \rho_E]] \}. \end{aligned} \quad (16)$$

* ywl@wipm.ac.cn

† guanhua@apm.ac.cn

‡ anjhong@lzu.edu.cn

It is easy to verify $Q_3 = 0$ according to Eq. (6). The

substitution of Eq. (4) into Eq. (14) results in

$$\begin{aligned}
Q_1 &= \sum_{\substack{\lambda, \lambda' = L, R \\ j, j' = 1, 2}} \int_0^t d\tau \int \frac{d\omega d\omega'}{2\pi} \delta(\omega - \omega') \delta_{\lambda, \lambda'} \{g_{\lambda' j'}(\omega') g_{\lambda j}^*(\omega) [\hat{m}_j \tilde{\rho}(t) \hat{m}_j^\dagger - \hat{m}_j^\dagger \hat{m}_j \tilde{\rho}(t)] e^{-i \frac{\omega' z_{j'}}{v_{\lambda'}} + i(\omega' - \omega_0)\tau} \\
&\quad \times e^{i \frac{\omega z_j}{v_\lambda} - i(\omega - \omega_0)t} + \text{H.c.}\} \\
&= \sum_{\substack{\lambda = L, R \\ j, j' = 1, 2}} \int_0^t d\tau \int \frac{d\omega}{2\pi} \{g_{\lambda j'}(\omega) g_{\lambda j}^*(\omega) [\hat{m}_j \tilde{\rho}(t) \hat{m}_j^\dagger - \hat{m}_j^\dagger \hat{m}_j \tilde{\rho}(t)] e^{i\omega_0(t-\tau)} e^{-i\omega(\frac{z_{j'} - z_j}{v_\lambda} + t - \tau)} + \text{H.c.}\}. \quad (17)
\end{aligned}$$

According to the Weisskopf-Wigner approximation, which is in the same accuracy as the Born-Markov approximation, $g_{\lambda l}(\omega)$ varies little around $g_{\lambda l}(\omega_0)$ for which the time integral in Eq. (17) is not negligible. We thus can replace $g_{\lambda l}(\omega)$ by $g_{\lambda l}(\omega_0)$ and the lower limit in the ω integration to $-\infty$ [1]. Further, by using the formula $\int \frac{d\omega}{2\pi} e^{\pm i\omega x} = \delta(x)$, Eq. (17) becomes

$$\begin{aligned}
Q_1 &= \sum_{\substack{\lambda = L, R \\ j, j' = 1, 2}} \int_0^t d\tau \delta(\tau - \frac{z_{j'} - z_j}{v_\lambda} - t) g_{\lambda j}(\omega_0) g_{\lambda j'}^*(\omega_0) \\
&\quad \times \{[\hat{m}_j \tilde{\rho}(t) \hat{m}_j^\dagger - \tilde{\rho}(t) \hat{m}_j^\dagger \hat{m}_j] e^{-i\omega_0(t-\tau)} + \text{H.c.}\}. \quad (18)
\end{aligned}$$

For the TE_{10} mode, the coupling strength becomes $g_{\lambda j}(\omega) = \sqrt{\frac{\gamma_0 M V_j}{2\epsilon_0 \omega a b}} [\frac{\pi}{a} \cos(\frac{\pi x_j}{a}) - k_\lambda \sin(\frac{\pi x_j}{a})]$ [2, 3], where a and b are the lengths of the cross section of the waveguide, ϵ_0 is the vacuum permittivity, and $k_\lambda = \omega/v_\lambda$ is the wave vector. We consider that the two YIG spheres have $x_1 = x_2 \equiv x_0$ and $V_1 = V_2 \equiv V$, which reduce $g_{\lambda 1}(\omega_0) = g_{\lambda 2}(\omega_0) \equiv g_\lambda(\omega_0)$. Further defining $v_R = -v_L \equiv v$, $\omega_0/v \equiv k_0$, $d \equiv z_2 - z_1$, and using the integration equality [4]

$$\int_{x_1}^{x_2} f(x) \delta(x - x_0) = \begin{cases} f(x_0), & x_0 \in (x_1, x_2) \\ \frac{f(x_0)}{2}, & x_0 = x_1 \text{ or } x_2 \\ 0, & x_0 > x_2 \text{ or } x_0 < x_1 \end{cases} \quad (19)$$

we derive

$$\begin{aligned}
Q_1 &= \sum_{\substack{\lambda = L, R \\ j = 1, 2}} \frac{\Gamma_\lambda}{2} [2\hat{m}_j \tilde{\rho}(t) \hat{m}_j^\dagger - \hat{m}_j^\dagger \hat{m}_j \tilde{\rho}(t) - \tilde{\rho}(t) \hat{m}_j^\dagger \hat{m}_j] \\
&\quad + \Gamma_R \{[\hat{m}_2 \tilde{\rho}(t) \hat{m}_1^\dagger - \tilde{\rho}(t) \hat{m}_1^\dagger \hat{m}_2] e^{-ik_0 d} + \text{H.c.}\} \\
&\quad + \Gamma_L \{[\hat{m}_1 \tilde{\rho}(t) \hat{m}_2^\dagger - \tilde{\rho}(t) \hat{m}_2^\dagger \hat{m}_1] e^{-ik_0 d} + \text{H.c.}\} \\
&= -i \left[\sum_{\lambda = L, R} \hat{H}_\lambda, \tilde{\rho}(t) \right] + \sum_{\lambda = L, R} \Gamma_\lambda \check{\mathcal{L}}_{\hat{M}_\lambda} \tilde{\rho}(t), \quad (20)
\end{aligned}$$

where $\Gamma_\lambda = g_\lambda(\omega_0)^2$ and $\check{\mathcal{L}}_{\hat{\sigma}} = \hat{\sigma} \cdot \hat{\sigma}^\dagger - \frac{1}{2} \{\hat{\sigma}^\dagger \hat{\sigma}, \cdot\}$ is the Lindblad superoperator. $\hat{H}_L = -\frac{i\Gamma_L}{2} (\hat{m}_1^\dagger \hat{m}_2 e^{ik_0 d} - \text{H.c.})$ and $\hat{H}_R = -\frac{i\Gamma_R}{2} (\hat{m}_2^\dagger \hat{m}_1 e^{ik_0 d} - \text{H.c.})$ describe the coherent coupling between the magnons mediated by the left- and

right-propagating electromagnetic fields. The operators $\hat{M}_L = \hat{m}_1 + \hat{m}_2 e^{ik_0 d}$ and $\hat{M}_R = \hat{m}_1 + \hat{m}_2 e^{-ik_0 d}$ describe the collective dissipations induced by the left- and right-propagating electromagnetic fields in the waveguide.

In a similar procedure as above, we derive

$$Q_2 = \sum_{j=1,2} \kappa \{(\bar{n} + 1) \check{\mathcal{L}}_{\hat{m}_j} + \bar{n} \check{\mathcal{L}}_{\hat{m}_j^\dagger}\} \tilde{\rho}(t), \quad (21)$$

with $\kappa \equiv |\chi(\omega_0)|^2$ and $\bar{n} \equiv \bar{n}_{\omega_0}$. Therefore, the master equation in the interaction picture becomes

$$\begin{aligned}
\dot{\tilde{\rho}}(t) &= -i[\hat{H}_d(t) + \sum_{\lambda=L,R} \hat{H}_\lambda, \tilde{\rho}(t)] + \left\{ \sum_{\lambda=L,R} \Gamma_\lambda \check{\mathcal{L}}_{\hat{M}_\lambda} \right. \\
&\quad \left. + \sum_{j=1,2} \kappa [(\bar{n} + 1) \check{\mathcal{L}}_{\hat{m}_j} + \bar{n} \check{\mathcal{L}}_{\hat{m}_j^\dagger}] \right\} \tilde{\rho}(t), \quad (22)
\end{aligned}$$

Going back to the Schrödinger picture, we obtain

$$\begin{aligned}
\dot{\rho}(t) &= -i[\hat{H}_m(t) + \sum_{\lambda=L,R} \hat{H}_\lambda, \rho(t)] + \left\{ \sum_{\lambda=L,R} \Gamma_\lambda \check{\mathcal{L}}_{\hat{M}_\lambda} \right. \\
&\quad \left. + \sum_{j=1,2} \kappa_j [(\bar{n} + 1) \check{\mathcal{L}}_{\hat{m}_j} + \bar{n} \check{\mathcal{L}}_{\hat{m}_j^\dagger}] \right\} \rho(t), \quad (23)
\end{aligned}$$

where $\hat{H}_m(t) = \sum_{j=1,2} \omega_0 (\hat{m}_j^\dagger \hat{m}_j + \frac{1}{2}) + \Omega (\hat{m}_1^\dagger e^{-i\omega_d t} + \text{H.c.})$.

II. DYNAMICAL SOLUTION

From the master equation (23), we obtain the closed equations of motion for the relevant operator moments

as

$$\frac{d\langle\hat{m}_1\rangle}{dt} = -\frac{\alpha}{2}\langle\hat{m}_1\rangle - \Gamma_L e^{ik_0 d}\langle\hat{m}_2\rangle - i\Omega, \quad (24)$$

$$\frac{d\langle\hat{m}_1^2\rangle}{dt} = -\alpha\langle\hat{m}_1^2\rangle - 2\Gamma_L e^{ik_0 d}\langle\hat{m}_1\hat{m}_2\rangle - 2i\Omega\langle\hat{m}_1\rangle, \quad (25)$$

$$\begin{aligned} \frac{d\langle\hat{m}_1^\dagger\hat{m}_1\rangle}{dt} &= -\alpha\langle\hat{m}_1^\dagger\hat{m}_1\rangle - (\Gamma_L e^{ik_0 d}\langle\hat{m}_1^\dagger\hat{m}_2\rangle \\ &\quad + i\Omega\langle\hat{m}_1^\dagger\rangle + \text{c.c.}) + \kappa\bar{n}, \end{aligned} \quad (26)$$

$$\frac{d\langle\hat{m}_2\rangle}{dt} = -\frac{\alpha}{2}\langle\hat{m}_2\rangle - \Gamma_R e^{ik_0 d}\langle\hat{m}_1\rangle, \quad (27)$$

$$\frac{d\langle\hat{m}_2^2\rangle}{dt} = -\alpha\langle\hat{m}_2^2\rangle - 2\Gamma_R e^{ik_0 d}\langle\hat{m}_1\hat{m}_2\rangle, \quad (28)$$

$$\begin{aligned} \frac{d\langle\hat{m}_2^\dagger\hat{m}_2\rangle}{dt} &= -\alpha\langle\hat{m}_2^\dagger\hat{m}_2\rangle - \Gamma_R (e^{ik_0 d}\langle\hat{m}_1\hat{m}_2^\dagger\rangle \\ &\quad + \text{c.c.}) + \kappa\bar{n}, \end{aligned} \quad (29)$$

$$\begin{aligned} \frac{d\langle\hat{m}_1\hat{m}_2\rangle}{dt} &= -\alpha\langle\hat{m}_1\hat{m}_2\rangle - \Gamma_R e^{ik_0 d}\langle\hat{m}_1^2\rangle \\ &\quad - \Gamma_L e^{ik_0 d}\langle\hat{m}_2^2\rangle - i\Omega\langle\hat{m}_2\rangle, \end{aligned} \quad (30)$$

$$\begin{aligned} \frac{d\langle\hat{m}_1^\dagger\hat{m}_2\rangle}{dt} &= -\alpha\langle\hat{m}_1^\dagger\hat{m}_2\rangle - \Gamma_R e^{ik_0 d}\langle\hat{m}_1^\dagger\hat{m}_1\rangle \\ &\quad - \Gamma_L e^{-ik_0 d}\langle\hat{m}_2^\dagger\hat{m}_2\rangle + i\Omega\langle\hat{m}_2\rangle, \end{aligned} \quad (31)$$

where $\alpha = \Gamma_L + \Gamma_R + \kappa$ and $\langle\cdot\rangle = \text{Tr}[\cdot\rho(t)]$. Consider that both the charger and the battery are initially prepared in the vacuum state $|0\rangle$. Consequently, the initial values of all the above moments are zero at $t = 0$.

We apply the Laplace transform $\mathcal{L}(f) = \int_0^\infty f(t)e^{-st} dt$ to Eqs. (24) and (27) and obtain

$$\mathcal{L}(\langle\hat{m}_1\rangle) = \frac{-i\Omega(s + \frac{\alpha}{2})}{s(s - s_+)(s - s_-)}, \quad (32)$$

$$\mathcal{L}(\langle\hat{m}_2\rangle) = \frac{i\Omega\Gamma_R e^{ik_0 d}}{s(s - s_+)(s - s_-)}. \quad (33)$$

where $s_\pm = -(\frac{1}{2}\alpha \pm \sqrt{\Gamma_L\Gamma_R e^{2ik_0 d}})$. The time-domain solutions are obtained by evaluating the inverse Laplace transforms via the residue theorem as

$$\langle\hat{m}_1\rangle = -i\Omega\left[\frac{\frac{\alpha}{2}}{s_+s_-} + \frac{(s_+ + \frac{\alpha}{2})e^{s_+t}}{s_+(s_+ - s_-)} + \frac{(s_- + \frac{\alpha}{2})e^{s_-t}}{s_-(s_- - s_+)}\right], \quad (34)$$

$$\langle\hat{m}_2\rangle = i\Omega\Gamma_R e^{ik_0 d}\left[\frac{1}{s_+s_-} + \frac{s_+^{-1}e^{s_+t}}{s_+ - s_-} + \frac{s_-^{-1}e^{s_-t}}{s_- - s_+}\right]. \quad (35)$$

In the long-time condition, we have their steady-state

form as

$$\langle\hat{m}_1\rangle_{ss} = \frac{-i\Omega\alpha/2}{s_+s_-} = \frac{-2i\Omega\alpha}{\alpha^2 - 4\Gamma_L\Gamma_R e^{2ik_0 d}}, \quad (36)$$

$$\langle\hat{m}_2\rangle_{ss} = \frac{i\Omega\Gamma_R e^{ik_0 d}}{s_+s_-} = \frac{4i\Omega\Gamma_R e^{ik_0 d}}{\alpha^2 - 4\Gamma_L\Gamma_R e^{2ik_0 d}}. \quad (37)$$

Next, we can prove that

$$\langle\hat{m}_l^2\rangle = \langle\hat{m}_l\rangle^2, \quad (38)$$

$$\langle\hat{m}_l^\dagger\hat{m}_l\rangle = |\langle\hat{m}_l\rangle|^2 + \kappa\bar{n}\mathcal{R}_l(t). \quad (39)$$

Proof. Performing the Laplace transform to Eqs. (25), (28), and (30), we obtain

$$\begin{aligned} \mathcal{L}(\langle\hat{m}_1^2\rangle) &= \frac{2i\Omega\Gamma_L e^{ik_0 d}}{(s + \alpha)^2 - 4\Gamma_L\Gamma_R e^{2ik_0 d}}[\mathcal{L}(\langle\hat{m}_2\rangle) \\ &\quad - \frac{[(s + \alpha)^2 - 2\Gamma_L\Gamma_R e^{2ik_0 d}]\mathcal{L}(\langle\hat{m}_1\rangle)}{\Gamma_L e^{ik_0 d}(s + \alpha)}], \end{aligned} \quad (40)$$

$$\mathcal{L}(\langle\hat{m}_2^2\rangle) = \frac{2i\Omega\Gamma_R e^{ik_0 d}[\mathcal{L}(\langle\hat{m}_2\rangle) - \frac{2\Gamma_R\mathcal{L}(\langle\hat{m}_1\rangle)}{(s + \alpha)e^{-ik_0 d}}]}{(s + \alpha)^2 - 4\Gamma_L\Gamma_R e^{2ik_0 d}}. \quad (41)$$

On the other hand, we derive the equations of $\langle\hat{m}_l\rangle \frac{d\langle\hat{m}_{l'}\rangle}{dt}$, with $l, l' \in \{1, 2\}$ from Eqs. (24) and (27). Then from their Laplace transforms and the property $\mathcal{L}(f \frac{df}{dt}) = \frac{s}{2}\mathcal{L}(f^2)$, we obtain

$$\begin{aligned} \frac{s}{2}\mathcal{L}(\langle\hat{m}_1\rangle^2) &= -\frac{\alpha}{2}\mathcal{L}(\langle\hat{m}_1\rangle^2) - \Gamma_L e^{ik_0 d}\mathcal{L}(\langle\hat{m}_1\rangle\langle\hat{m}_2\rangle) \\ &\quad - i\Omega\mathcal{L}(\langle\hat{m}_1\rangle), \end{aligned} \quad (42)$$

$$\begin{aligned} \frac{s}{2}\mathcal{L}(\langle\hat{m}_2\rangle^2) &= -\frac{\alpha}{2}\mathcal{L}(\langle\hat{m}_2\rangle^2) - \Gamma_R e^{ik_0 d}\mathcal{L}(\langle\hat{m}_1\rangle\langle\hat{m}_2\rangle), \quad (43) \\ s\mathcal{L}(\langle\hat{m}_1\rangle\langle\hat{m}_2\rangle) &= -\alpha\mathcal{L}(\langle\hat{m}_1\rangle\langle\hat{m}_2\rangle) - \Gamma_R e^{ik_0 d}\mathcal{L}(\langle\hat{m}_1\rangle^2) \\ &\quad - \Gamma_L e^{ik_0 d}\mathcal{L}(\langle\hat{m}_2\rangle^2) - i\Omega\mathcal{L}(\langle\hat{m}_2\rangle), \end{aligned} \quad (44)$$

They readily result in

$$\begin{aligned} \mathcal{L}(\langle\hat{m}_1\rangle^2) &= \frac{2i\Omega\Gamma_L e^{ik_0 d}}{(s + \alpha)^2 - 4\Gamma_L\Gamma_R e^{2ik_0 d}}[\mathcal{L}(\langle\hat{m}_2\rangle) \\ &\quad - \frac{[(s + \alpha)^2 - 2\Gamma_L\Gamma_R e^{2ik_0 d}]\mathcal{L}(\langle\hat{m}_1\rangle)}{\Gamma_L e^{ik_0 d}(s + \alpha)}], \end{aligned} \quad (45)$$

$$\mathcal{L}(\langle\hat{m}_2\rangle^2) = \frac{2i\Omega\Gamma_R e^{ik_0 d}[\mathcal{L}(\langle\hat{m}_2\rangle) - \frac{2\Gamma_R\mathcal{L}(\langle\hat{m}_1\rangle)}{(s + \alpha)e^{-ik_0 d}}]}{(s + \alpha)^2 - 4\Gamma_L\Gamma_R e^{2ik_0 d}}, \quad (46)$$

which matches Eq. (41) exactly. Therefore, we have $\langle\hat{m}_l^2\rangle = \langle\hat{m}_l\rangle^2$ after the inverse Laplace transform.

Performing the Laplace transform to Eqs. (26), (29), and (31), we obtain

$$\mathcal{L}(\langle \hat{m}_1^\dagger \hat{m}_1 \rangle) = \frac{\Omega[i(s+\alpha)\mathcal{L}(\langle \hat{m}_1 \rangle) - i\Gamma_L e^{ik_0d}\mathcal{L}(\langle \hat{m}_2 \rangle) + \text{c.c.}] + 2\Gamma_L^2 \mathcal{L}(\langle \hat{m}_2^\dagger \hat{m}_2 \rangle) + \frac{\kappa\bar{n}(s+\alpha)}{s}}{(s+\alpha)^2 - 2\Gamma_L\Gamma_R \cos(2k_0d)}, \quad (47)$$

$$\begin{aligned} \mathcal{L}(\langle \hat{m}_2^\dagger \hat{m}_2 \rangle) &= \frac{\Omega\Gamma_R}{[(s+\alpha)^2 - 2\Gamma_L\Gamma_R \cos(2k_0d)]^2 - 4\Gamma_L^2\Gamma_R^2} \{ [2\Gamma_L\Gamma_R \sin(2k_0d) - i(s+\alpha)^2] e^{-ik_0d} \mathcal{L}(\langle \hat{m}_2 \rangle) \\ &\quad + 2i\Gamma_R(s+\alpha)\mathcal{L}(\langle \hat{m}_1 \rangle) + \text{c.c.} \} + \frac{\kappa\bar{n}(s+\alpha)[(s+\alpha)^2 - 2\Gamma_L\Gamma_R \cos(2k_0d) + 2\Gamma_R^2]}{s\{[(s+\alpha)^2 - 2\Gamma_L\Gamma_R \cos(2k_0d)]^2 - 4\Gamma_L^2\Gamma_R^2\}}. \end{aligned} \quad (48)$$

On the other hand, from the Laplace transforms of Eqs. (24) and (27), we have

$$\mathcal{L}(|\langle \hat{m}_1 \rangle|^2) = \frac{\Omega[i(s+\alpha)\mathcal{L}(\langle \hat{m}_1 \rangle) - i\Gamma_L e^{ik_0d}\mathcal{L}(\langle \hat{m}_2 \rangle) + \text{c.c.}] + 2\Gamma_L^2 \mathcal{L}(|\langle \hat{m}_2 \rangle|^2)}{(s+\alpha)^2 - 2\Gamma_L\Gamma_R \cos(2k_0d)}, \quad (49)$$

$$\mathcal{L}(|\langle \hat{m}_2 \rangle|^2) = \frac{\Omega\Gamma_R\{[2\Gamma_L\Gamma_R \sin(2k_0d) - i(s+\alpha)^2] e^{-ik_0d} \mathcal{L}(\langle \hat{m}_2 \rangle) + 2i\Gamma_R(s+\alpha)\mathcal{L}(\langle \hat{m}_1 \rangle) + \text{c.c.}\}}{[(s+\alpha)^2 - 2\Gamma_L\Gamma_R \cos(2k_0d)]^2 - 4\Gamma_L^2\Gamma_R^2}. \quad (50)$$

The comparison of Eqs. (47, 48) and Eqs. (49, 50) leads to

$$\mathcal{L}(\langle \hat{m}_l^\dagger \hat{m}_l \rangle) = \mathcal{L}(|\langle \hat{m}_l \rangle|^2) + \kappa\bar{n}\mathcal{T}_l, \quad (51)$$

with

$$\mathcal{T}_{1/2} = \frac{(s+\alpha)[2\Gamma_{L/R}^2 + (s+\alpha)^2 - 2\Gamma_L\Gamma_R \cos(2k_0d)]}{s\{[(s+\alpha)^2 - 2\Gamma_L\Gamma_R \cos(2k_0d)]^2 - 4\Gamma_L^2\Gamma_R^2\}} \quad (52)$$

Making the inverse Laplace transform to Eq. (51), we obtain Eq. (39), with $\mathcal{R}_l(t)$ being the inverse Laplace transform of \mathcal{T}_l . ■

In the following, we evaluate $\mathcal{R}_l(t)$. Its definition is

$$\mathcal{R}_l(t) = \sum_{i=1,4,5,6,7} \text{Res}_{s=s_i} [\mathcal{T}_l(s)e^{st}], \quad (53)$$

The poles of $\mathcal{T}_l(s)$ are determined by the equation $s\{[(s+\alpha)^2 - 2\Gamma_L\Gamma_R \cos(2k_0d)]^2 - 4\Gamma_L^2\Gamma_R^2\} = 0$, which gives

$$s_1 = 0, \quad (54)$$

$$s_{4/5} = -\alpha + \sqrt{2\Gamma_L\Gamma_R[\cos(2k_0d) \pm 1]}, \quad (55)$$

$$s_{6/7} = -\alpha - \sqrt{2\Gamma_L\Gamma_R[\cos(2k_0d) \pm 1]}. \quad (56)$$

According to the residue theorem, we obtain $\mathcal{R}_l(t)$ straightforwardly. Their steady-state solutions in the long-time limit read

$$\mathcal{R}_{1/2,ss} = \frac{\alpha[\alpha^2 - 2\Gamma_L\Gamma_R \cos(2k_0d) + 2\Gamma_{L/R}^2]}{(\alpha^2 - 2\Gamma_L\Gamma_R \cos(2k_0d))^2 - 4\Gamma_L^2\Gamma_R^2}. \quad (57)$$

III. ENERGIES AND ERGOTROPY

The elements of the covariance matrix $\sigma^{(j)}(t)$ and the mean vector $\mathbf{d}^{(j)}(t)$ of the charger for $j = 1$ and the QB for $j = 2$ are $\sigma_{lm}^{(j)} = \text{Tr}\{\Delta\hat{r}_l, \Delta\hat{r}_m\}\rho_j(t)$ and $d_l^{(j)} = \text{Tr}[\hat{r}_l^{(j)}\rho_j(t)]$, with $\Delta\hat{r}_l^{(j)} = \hat{r}_l^{(j)} - d_l^{(j)}$ and $\hat{r}^{(j)} =$

$(\frac{\hat{m}_j^\dagger + \hat{m}_j}{\sqrt{2}}, \frac{\hat{m}_j - \hat{m}_j^\dagger}{i\sqrt{2}})^\top$. Thus, we have

$$d_1^{(j)}(t) = \langle \hat{m}_j \rangle / \sqrt{2} + \text{c.c.}, \quad (58)$$

$$d_2^{(j)}(t) = \langle \hat{m}_j \rangle / (i\sqrt{2}) + \text{c.c.}, \quad (59)$$

$$\begin{aligned} \sigma_{11}^{(j)}(t) &= \langle \hat{m}_j^2 \rangle + \langle \hat{m}_j^{\dagger 2} \rangle + 2\langle \hat{m}_j^\dagger \hat{m}_j \rangle + 1 \\ &\quad - \langle \hat{m}_j \rangle^2 - 2|\langle \hat{m}_j \rangle|^2 - \langle \hat{m}_j^\dagger \rangle^2 \\ &= 2\kappa\bar{n}\mathcal{R}_j(t) + 1, \end{aligned} \quad (60)$$

$$\sigma_{12}^{(j)}(t) = \frac{1}{i}[\langle \hat{m}_j^2 \rangle - \langle \hat{m}_j^{\dagger 2} \rangle - \langle \hat{m}_j \rangle^2 + \langle \hat{m}_j^\dagger \rangle^2] = 0, \quad (61)$$

$$\begin{aligned} \sigma_{22}^{(j)}(t) &= -\langle \hat{m}_j^2 \rangle - \langle \hat{m}_j^{\dagger 2} \rangle + 2\langle \hat{m}_j^\dagger \hat{m}_j \rangle + 1 \\ &\quad + \langle \hat{m}_j \rangle^2 - 2|\langle \hat{m}_j \rangle|^2 + \langle \hat{m}_j^\dagger \rangle^2 \\ &= 2\kappa\bar{n}\mathcal{R}_j(t) + 1, \end{aligned} \quad (62)$$

where Eqs. (38) and (39) have been used. Substituting them into the expressions of energy of the charger and the QB and the ergotropy of the QB, we obtain

$$\begin{aligned} \mathcal{E}_{C/B}(t) &= \omega_0\{\text{Tr}[\sigma^{(1/2)}(t)]/4 + |\mathbf{d}^{(1/2)}(t)|^2/2\} \\ &= \omega_0[|\langle \hat{m}_{1/2} \rangle|^2 + \kappa\bar{n}\mathcal{R}_{1/2}(t) + \frac{1}{2}], \end{aligned} \quad (63)$$

$$\mathcal{W}(t) = \mathcal{E}_B(t) - \omega_0\sqrt{\det[\sigma^{(2)}(t)]}/2 = \omega_0|\langle \hat{m}_2 \rangle|^2. \quad (64)$$

At zero temperature ($\bar{n} = 0$), Eq. (63) reduces to $\lim_{T \rightarrow 0} \mathcal{E}_{C/B}(t) = \omega_0(|\langle \hat{m}_{1/2} \rangle_{ss}|^2 + \frac{1}{2})$ in the long-time condition.

IV. EFFECT OF THE DRIVING STRENGTH

In the main text, our results show an enhancement factor of approximately 34 for $\mathcal{E}_{ss|D=1}/\mathcal{E}_{ss|D=0}$. Here we further demonstrate that increasing the driving strength raises this enhancement factor until it saturates at around 55. Figure 1(a) plots the $\mathcal{E}_{ss|D=1}/\mathcal{E}_{ss|D=0}$ as a function of distance k_0d under different driving strengths Ω . The $\mathcal{E}_{ss|D=1}/\mathcal{E}_{ss|D=0}$ increases with the

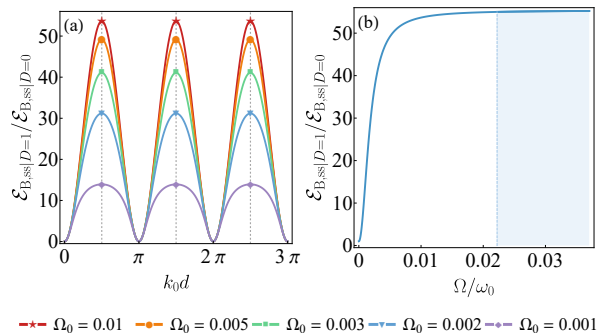


FIG. 1. (a) $\mathcal{E}_{ss|D=1}/\mathcal{E}_{ss|D=0}$ as a function of the normalized distance k_0d for different driving strengths. (b) $\mathcal{E}_{ss|D=1}/\mathcal{E}_{ss|D=0}$ versus driving strength at a fixed distance $k_0d = \pi/2$. The parameters are $\Gamma_R \approx 0.001\omega_0$, $\bar{n} = 0$, $\kappa = \frac{\Gamma_R}{20}$, and $\Omega_0 = \Omega/\omega_0$.

driving strength and exhibits a periodic dependence on k_0d , reaching its maximum at $d = (n + 1/2)\pi/k_0$. Figure 1(b) shows the variation of the $\mathcal{E}_{ss|D=1}/\mathcal{E}_{ss|D=0}$ with the driving strength at the fixed distance $d = \pi/2k_0$. The $\mathcal{E}_{ss|D=1}/\mathcal{E}_{ss|D=0}$ grows with the driving strength and eventually saturates at an enhancement factor of approximately 55. This indicates that the energy enhancement can be improved by increasing the driving strength. However, according to Eq. (12) in the main text, the enhancement factor of the extractable work is independent of the driving strength.

-
- [1] M. O. Scully and M. S. Zubairy, in *Quantum Optics* (Cambridge University Press, 1997).
 - [2] T. Yu, Y.-X. Zhang, S. Sharma, X. Zhang, Y. M. Blanter, and G. E. W. Bauer, Magnon accumulation in chirally coupled magnets, *Phys. Rev. Lett.* **124**, 107202 (2020).
 - [3] T. Yu, X. Zhang, S. Sharma, Y. M. Blanter, and G. E. W. Bauer, Chiral coupling of magnons in waveguides, *Phys. Rev. B* **101**, 094414 (2020).
 - [4] S. M. Barnett and P. M. Radmore, *Methods in Theoretical Quantum Optics* (Oxford University Press, 2002).